Tetrahedron 75 (2019) 3118–3127

Contents lists available at ScienceDirect

Tetrahedron

journal homepage: www.elsevier.com/locate/tet

Steric effects of bulky tethered arylpiperazines on the reactivity of Co-Schiff base oxidation catalysts—a synthetic and computational study

Rebecca E. Key [a], Thomas Elder [b], Joseph J. Bozell [a, *]

[a] Center for Renewable Carbon, Center for Direct Catalytic Conversion of Biomass to Biofuels (C3Bio), University of Tennessee, 2506 Jacob Drive, Knoxville, TN 37996, USA
[b] USDA Forest Service, Forest Operations Research, 521 Devall Drive, Auburn, AL 36849, USA

ARTICLE INFO

Article history:
Received 9 January 2019
Received in revised form
23 April 2019
Accepted 24 April 2019
Available online 30 April 2019

Keywords:
Phenolic oxidation
Lignin
Lignin models
Arylpiperazine base tethers
Co-Schiff base
Renewable carbon

ABSTRACT

New C2-symmetric and C2-asymmetric Co-Schiff base catalysts tethered to arylpiperazine units were synthesized and used to oxidize phenolic lignin models to *para*-benzoquinones. Synthetic approaches to these catalysts were optimized to include fewer steps and broaden the types of catalyst structures available. In contrast to conventional Co-Schiff base catalysts, these systems induce phenolic oxidation in the absence of an external axial base, simplifying the process. Asymmetric catalysts bearing a phenylethylene or diphenylmethyl piperazine substituent display the highest catalytic activity observed to date for the conversion of S-models to 2,6-dimethoxybenzoquinone (DMBQ). Computational analysis shows that more reactive catalysts populate conformations that favor oxidation in preference to non-productive decomposition routes. This balance between catalyst reactivity and catalyst deactivation is optimized by inclusion of sufficient steric bulk around the periphery of the Schiff base ligand, reducing catalyst deactivation and allowing oxidations to proceed in the absence of an added axial ligand.

1. Introduction

Recent years have seen a dramatic increase in efforts to understand and control the reactivity of lignin as a low cost and exceptionally abundant source of renewable carbon. Nonetheless, lignin's structural heterogeneity continues to frustrate development of chemoselective catalysts for its conversion to high value biobased chemicals [1–6]. These challenges are amplified when biorefining converts *native* lignin (lignin as found in a raw material's lignocellulosic matrix) into *technical* lignin (lignin isolated as a separate process stream). This transformation introduces a wide range of additional structural changes that depend on the methodology and severity of the biorefining process [7–11]. For example, multiple catalytic processes have targeted cleavage of the β-O-4 unit, the primary interunit linkage in native lignin [12–18]. We have described how such transformations are not suitable for technical lignin generated within the biorefinery, as typical lignin isolation processes greatly reduce or eliminate this linkage [7,19–22]

Newer "lignin first" approaches have addressed this challenge through the use of whole biomass and its contained native lignin as a feedstock. Recent improvements in catalytic hydrogenolysis processes first developed in the 1940s give lignin-derived products enriched in low molecular weight aromatics [23]. Ni/Al_2O_3 catalyzes the hydrogenation of lignin in birch wood to an oil containing a high proportion of *n*-propanolguaiacol and -syringol [24]. Catalytic systems based on Pd/C/Zn and Ni/C selectively afford a small number of propylphenols at 50–60% conversion of model lignin polymers or the lignin in *Miscanthus* [25,26]. Catalytic Ni/C gives 89% selectivity for the hydrogenolysis of the lignin in birch sawdust to propylsyringol and propylguaiacol at 54% lignin conversion. However, the failure of these and additional studies to improve these yields suggests that a maximum conversion limitation may exist for reductive lignin depolymerization processes [27].

Moreover, the continuing focus on biofuel development in the biorefining industry indicates that technical lignin isolated from well-recognized biomass fractionation processes (e. g., dilute acid, steam explosion, organosolv) will likely remain the standard [28]. Thus, catalytic conversion methodology for technical lignin must be able to accommodate the structural changes that result from these types of processing. For example, cleavage of lignin's β-O-4 linkage during biorefining simultaneously generates a markedly higher proportion of free phenolic groups (7–70%) than are present in native material [29]. Further, the substituted aromatics present in

* Corresponding author.
E-mail address: jbozell@utk.edu (J.J. Bozell).

https://doi.org/10.1016/j.tet.2019.04.059
0040-4020/

technical lignin retain the electron-rich character of native lignin, making them susceptible to selective oxidation. Accordingly, we have focused on catalytic oxidation of lignin-like phenols as the best model of the lignin that will be available as a renewable carbon source from the biorefinery.

Specifically, we have examined lignin and lignin model oxidation catalyzed by Co-Schiff base complexes (e. g., Co(salen) **1**, Scheme 1) using molecular oxygen as the terminal oxidant [19,20,30,31]. These catalysts have known utility in the oxidation of simple phenols unsubstituted in the *para*-position to the corresponding *para*-benzoquinones [32–38]. We demonstrated that Co-Schiff base catalyzed oxidation of a series of lignin-like *para*-substituted phenols also afford *para*-benzoquinones [30], likely following the mechanism shown in Scheme 1 [35,36,39]

An external ligand, such as a substituted pyridine or imidazole, binds to the axial position on Co and promotes the formation of Co-superoxo complex **2** [35,40,41]. Complex **2** removes a phenolic hydrogen from the substrate to give phenoxy radical **3**, initiating a process that ultimately leads to the production of *para*-benzoquinones [35,40–47]. We reported the first examples of this transformation and showed that syringyl (S) lignin models were converted in good yield to dimethoxybenzoquinone (DMBQ, **4**), but the corresponding conversion of guaiacyl (G) models to monomethoxybenzoquinone (MMBQ, **5**) proceeded in markedly lower yields [30]. Subsequent work revealed that the yield of **5** from vanillyl alcohol increased when the reaction was supplemented with a sterically hindered, non-coordinating aliphatic base, such as DIPEA. These results can be attributed to the hindered base deprotonating the phenol and forming a more oxidizable phenolate ion **6**, giving a more rapid formation of the phenoxy radical **3** [31].

Based on these results, we developed a family of second-generation, asymmetric (i.e., no C_2 symmetry) Co-Schiff base catalysts that placed the sterically hindered base (in the form of a substituted piperazine) in closer proximity to the Co center by incorporating it into the Schiff base ligand itself (e. g., **7** and **8**, Scheme 1). In particular, complex **7** effectively catalyzed the high yield oxidation of S and G monolignol models, as well as *S,S*- and *S,G*-dimeric models (Fig. 1) to the corresponding *para*-benzoquinones, in less time and using half the catalyst loading of earlier studies [19]. Of particular interest was that the increased reactivity of the second generation catalysts occurred in the *absence* of an external axial base, in marked contrast to oxidations carried out with the structurally simpler **1** and many related catalysts. This observation suggested that the increased steric bulk of catalysts **7** or **8** was a critical factor in improving the known balance between catalyst reactivity and catalyst deactivation [48–50]. As part of our effort to understand the fundamental features that control the reactivity of Co-Schiff base oxidation catalysts, we wish to report

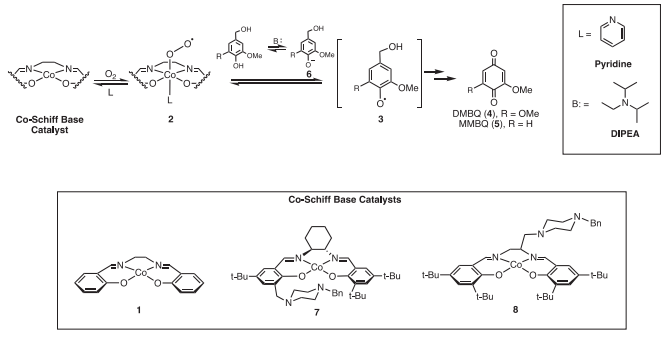

Scheme 1. Mechanism of the Co-Schiff base-catalyzed oxidation of *para*-substituted phenols with oxygen.

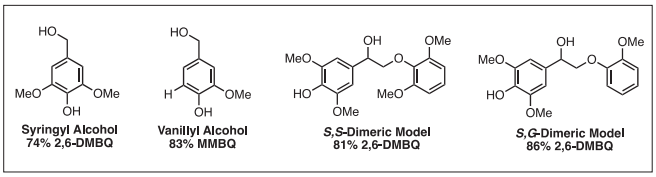

Fig. 1. S- and G-type lignin models and dimeric lignin models examined with second-generation Co-Schiff base catalyst **7**.

synthetic and computational results for a family of new, sterically hindered Co-Schiff base complexes.

2. Results and discussion

2.1. The role of sterics in M-Schiff base-catalyzed reactions

The accepted model for binding of O_2 to a Co-Schiff base complex postulates that the interaction of the catalyst and an external base raises the energy of the metal dz^2 orbital sufficiently to overlap with appropriate orbitals on O_2 [51–53]. Since our complexes catalyzed oxidation of lignin model phenols to quinones in the absence of base, we compared the relative dz^2 orbital energies of several Co-Schiff base complexes examined in this study [54] to previous results for Co(salen) **1** in the presence and absence of common ligands using the B3LYP density functional method and the 6-31G(d) basis set (Fig. 2).

As expected, the evaluation supports lower dz^2 energies for Co(salen) **1** in the presence of weaker ligands (e. g., DMF) and significantly higher dz^2 energies in the presence of strong ligands (e. g., N-Me imidazole, N,N-diMe piperazine, DMAP). Moreover, the evaluation is well ordered, in that the dz^2 energy is lowest for Co(salen) in the absence of a ligand and rises predictably in the presence of increasingly stronger ligands. Accordingly, and consistent with the literature, Co(salen) is also an excellent phenol oxidation catalyst in the presence of strong ligands. Our early studies showed that attempting oxidation of substituted phenols with simple Co(salen) in the absence of an external ligand failed to generate the quinone product and led to the formation of a catalytically inactive complex [30].

Of particular interest, however, is that some catalysts (**S1**, **S2**, [Supporting Information]; **12**, **13**) with low calculated dz^2 orbital energies still serve as oxidation catalysts for substituted phenols. **S2**, **12**, and **13** give moderate to good yields of DMBQ from syringyl

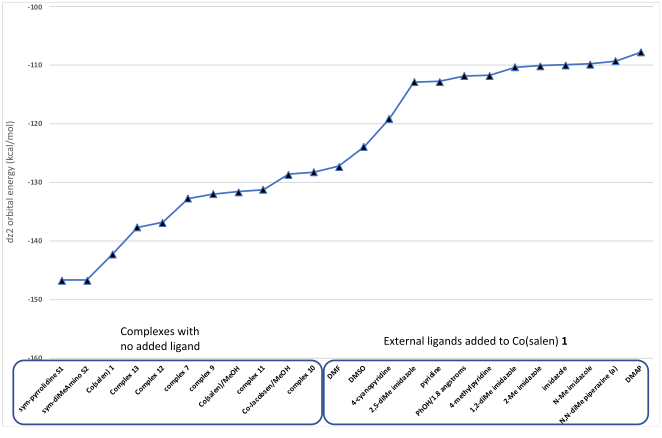

Fig. 2. Calculated relative dz^2 orbital energies for a series of ligated and non-ligated Co-Schiff base catalysts; [a]Modeling carried out with Co-Jacobsen catalyst (Supplemental Information).

alcohol. Further, our earlier work showed that the piperazine substituent in complex **7** was not within binding distance to the Co center [20]. We therefore suspected that the introduction of sterically bulky groups on the catalyst was reducing or slowing catalyst deactivation pathways rather than promoting formation of Co-superoxo complex **2**.

The literature reports several examples of the influence of sterics on the reactivity of metal-Schiff base catalysts. For example, Pospisil et al. synthesized various Mn-Jacobsen catalysts and examined their catalytic activity in olefin epoxidation. They observed that higher *ee*s were observed when bulky *tert*-butyl groups were present on the catalysts, as these groups effectively limit substrate approaches to a trajectory that favors formation of a single enantiomer [55,56]. Higher catalytic activity in ring-opening polymerization of *rac*- and L-lactide was observed when less sterically hindered Al(salen) catalysts were used, while higher stereoselectivities were observed with more sterically hindered catalysts [57]. An increase in the steric bulk of Cr(salen) complexes resulted in a higher yield and *ee* of cycloadducts in oxo-Diels-Alder reactions when compared to the less hindered Cr-Jacobsen catalyst [58]. In our work, the introduction of *tert*-butyl groups on the catalyst is thought to reduce catalyst deactivation that occurs via formation of Co-peroxo dimers seen in simpler Co(salen) systems [41,46,47]. Therefore, our catalyst design targeted optimizing the steric bulk environment of several piperazine-tethered-Co-Schiff base catalysts to maximize interactions between catalyst, base, and substrate while minimizing catalyst deactivation.

2.2. Syntheses of arylpiperazine-tethered Co-Schiff base catalysts

The family of new catalysts synthesized for this study is shown in Fig. 3. Both C_2 symmetric and C_2 asymmetric ligands were prepared, incorporating differing side chains at the piperazine moiety, exemplifying both increased steric bulk (**9**, **11**, **12** and **13**) and increased chain length (**10** and **13**).

Symmetric catalysts **12** and **13** (Scheme 2) were prepared by condensing one equivalent of (±)-*trans*-1,2-diaminocyclohexane (**19**) and two equivalents of either arylpiperazine salicylaldehyde **17** or **18** to give ligands **24** and **25** in moderate and high yields, respectively. Metallation of **24** and **25** with $Co(OAc)_2 4H_2O$ provided Co-Schiff base catalysts **12** and **13**. Asymmetric catalysts **9** and **10** were synthesized in a similar manner but required protecting one of the amine groups of **19** as the HCl salt **20** [59,60]. One-pot condensation of the free amine in **20** with one equivalent of **21** followed by deprotonation and then condensation of the intermediate with one equivalent of either **17** or **18** afforded moderate yields of Schiff base ligands **22** and **23**, respectively [19,59].

The commercial availability of the diphenylmethyl and

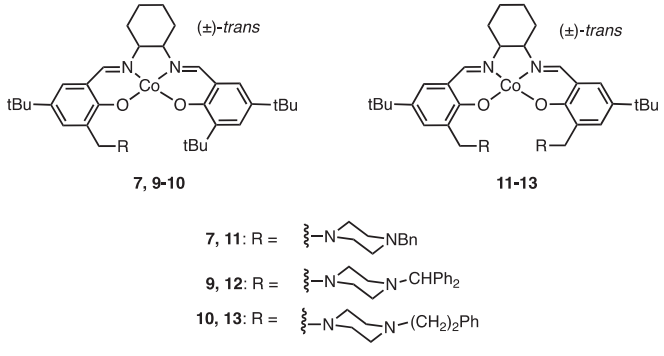

Fig. 3. C_2 Symmetric and C_2 asymmetric Co-Schiff base catalysts evaluated in this study.

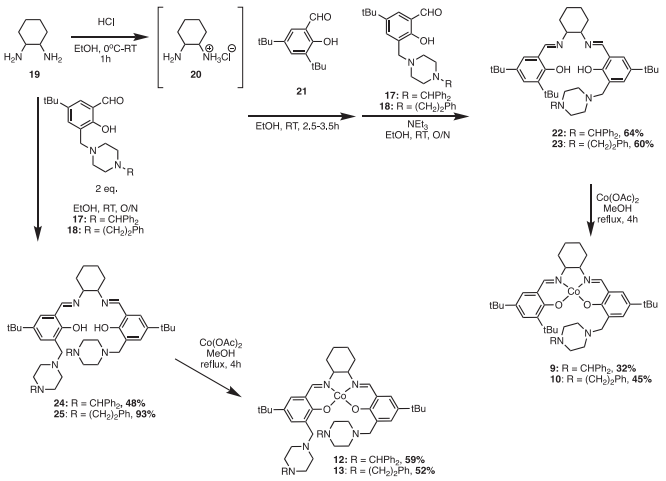

Scheme 2. Synthesis of arylpiperazine-tethered Co-Schiff base catalysts **9**–**10** and **12**–**13**.

phenethyl substituted piperazines give the advantage of simplifying the synthesis of ligands **22**–**25**. Metallation of **22** and **23** using $Co(OAc)_2 4H_2O$ provided asymmetric catalysts **9** and **10**, respectively. The low yields for catalysts **9** and **12** are likely the result of forcing bulky substituents into proximity as the ligand adopts a square planar conformation upon insertion of the Co.

2.3. Arylpiperazine-tethered Co-Schiff base-catalyzed oxidation of S-lignin models

The reactivity of catalysts **9**–**13** was evaluated at different reaction times in MeOH solvent for the oxidation of syringyl alcohol and α-methylsyringyl alcohol to DMBQ. The results were compared to compound **7**, the most active Co-Schiff base catalyst to date (Table 1, entries 1 and 2). Overall, the catalysts give good yields of DMBQ, accompanied by smaller amounts (<10%) of the corresponding aldehyde arising from oxidation of the benzylic alcohol. In addition, the asymmetric catalysts give generally higher yields of quinone than the symmetric catalysts, reflecting the impact of greater steric bulk on the oxidation process. In all cases, the catalysts operated successfully without the addition of an external axial base.

Asymmetric catalyst **9**, bearing a single diphenylmethyl (diPhMe) piperazine substituent, produced DMBQ in 70 and 81% yield at 18 h and 1 h reaction times, respectively (Table 1, entries 3 and 4), comparable to catalyst **7** (Table 1, entries 1 and 2). Both **7** and **9** gave DMBQ in slightly lower yields at longer reaction times. The reason for these lower DMBQ yields at longer reaction times is not clear but may suggest that the quinone product is being consumed in a slower reaction process. Related work in our group has revealed that the quinone product may inhibit the oxidation through the formation of intermediate Co-quinone complexes. Over long reaction times, a Co-DMBQ complex may be forming slowly [61]. Asymmetric catalyst **10**, bearing a phenethyl side chain, catalyzed the formation of DMBQ in comparable yields to **7** and **9** (Table 1, entries 5 and 6) when oxidations were run overnight, and comparable yields (73%, Table 1, entry 6) when run for 1 h.

In some cases, a further increase in the steric bulk of the catalysts resulting from the introduction of two large substituents onto the Schiff base ligand decreased the quinone yield (Table 1, entries 9–11). Surprisingly, introduction of a second, large diPhMe-group (catalyst **12**) had little impact on the yield of DMBQ, with yields of 73 and 74% at 18 h and 1 h reaction times, respectively (Table 1,

Table 1
Arylpiperazine-tethered Co-Schiff base-catalyzed oxidation of S models in MeOH.

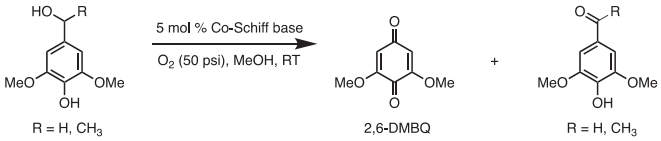

Entry	Catalyst	R	Reaction Time (h)	DMBQ yield (%)	Aldehyde yield (%)
1	**7**, asym-NBn	H	18	71[a]	4[a]
2	**7**, asym-NBn	H	1	75[b]	1[a]
3	**9**, asym-diPhMe	H	18	70[b,c]	6[a,c]
4	**9**, asym-diPhMe	H	1	81[b,c]	4[a,c]
5	**10**, asym-Phenethyl	H	18	80[b,c]	7[b,c]
6	**10**, asym-Phenethyl	H	1	73[a–c]	7[a–c]
7	**12**, sym-diPhMe	H	18	73[a,c]	3[a,c]
8	**12**, sym-diPhMe	H	1	74[a,c]	4[a,c]
9	**11**, sym-NBn	H	18	67[a–c]	4[a,c]
10	**11**, sym-NBn	H	1	64[a,c]	9[a,c]
11	**13**, sym-Phenethyl	H	18	52[a,c]	9[a,c]
12	**7**, asym-NBn	CH_3	16	73[d]	–
13	**9**, asym-diPhMe	CH_3	16	76[d]	–
14	**10**, asym-Phenethyl	CH_3	16	77[b]	1[a,c]
15	**11**, sym-NBn	CH_3	16	80[c,d]	–
16	**12**, sym-diPhMe	CH_3	16	73[c,d]	–

Mol % is calculated relative to the substrate; diPhMe: 1-diphenylmethyl; Phenethyl: 1-phenethyl.
[a] Yields obtained via ^{1}H NMR integration.
[b] Combined yield from isolated and ^{1}H NMR integration.
[c] Denotes the average yields between two runs; [d]Isolated yield.

entries 7 and 8). Interestingly, symmetric phenethyl catalyst **13** gave noticeably lower yields of DMBQ (52%, Table 1, entry 11) when compared to all other catalysts tested, contrasting the results obtained with its asymmetric counterpart **10**. The presence of a single phenethyl group appears to provide the steric bulk necessary to generate an active catalyst, but the presence of two phenethyl groups and their longer tethers may afford catalyst conformations that impede access of the substrate to the Co center.

We also evaluated the activity of catalysts **9**–**12** with α-methylsyringyl alcohol and compared the results to oxidations using catalyst **7** (Table 1, entries 12–16). Overall, the trends were very similar to oxidation of syringyl alcohol. Oxidation using catalyst **7** provided yields of DMBQ comparable to previously reported results [19] (73%, Table 1, entry 12). Catalyst **9** gave yields of DMBQ that were similar to catalyst **7** (76%, Table 1, entry 13). Catalyst **10**, the most active catalyst for the oxidation of syringyl alcohol at long reaction times, performed similarly, providing DMBQ in slightly higher yield (77%, Table 1, entry 14) than catalyst **7**. Catalyst **12** provided DMBQ in yields equivalent to catalyst **7** (73%, Table 1, entry 16), again showing that the addition of a second diPhMe-piperazine substituent has little effect on the oxidation. Since the catalysts enable oxidation in the absence of a strong axial ligand, we assume that the axial position is filled with a more weakly binding ligand, such as the MeOH solvent used in the reaction. While simple Co(salen) **1** preferentially deactivates in the absence of an added base, the presence of large groups on the periphery of the second generation catalysts induces an inhibition of catalyst deactivation and enables reaction in the absence of an additional axial ligand. Although the ability of MeOH to raise the energy of the dz^2 orbital on Co is much lower than pyridine, it may be sufficient to generate enough catalytically active Co-superoxo intermediate to carry the oxidation of S model substrates as long as deactivation processes are inhibited.

To examine the effect of solvent on oxidation, we examined the activity of catalysts **10** and **13** for the oxidation of syringyl alcohol oxidation in dichloromethane (DCM) and compared the results to catalyst **7** (Table 2). DCM, a non-coordinating solvent, should not bind to the Co-center, thus inhibiting the formation of the catalytically active Co-superoxo complex, and reducing the yield of DMBQ in comparison to reactions performed in MeOH. Indeed, all catalysts evaluated for oxidative activity in DCM provided lower yields of DMBQ when compared to their activity in methanol. Specifically, catalyst **7** gave DMBQ in 53% yield (Table 2, entry 1). Catalyst **10** gave a yield significantly lower yield of DMBQ in DCM when compared to MeOH (26%, Table 2, entry 2). Catalyst **13**, which also gave lower yields in MeOH, gave a 38% yield of MMBQ in DCM (Table 2, entry 3).

In DCM a decrease in DMBQ is accompanied by an increase in syringaldehyde when compared to the oxidations in methanol. Thus, the yield of DMBQ in methanol could be due, in part, to the conversion of intermediate syringaldehyde to DMBQ. To further investigate this, oxidations of syringaldehyde in both methanol and DCM were compared using catalyst **7**. The yield of DMBQ from syringaldehyde is higher in methanol (29%) than in DCM (3%). Therefore, it can be concluded that higher yields of DMBQ from oxidations run in methanol result from the oxidation of both syringyl alcohol and syringaldehyde, whereas the DMBQ yield from the oxidations run in DCM result from the conversion of syringyl alcohol [30].

2.4. Arylpiperzine-tethered Co-Schiff base-catalyzed oxidation of G-lignin models

The reactivity of the catalysts toward vanillyl alcohol as a model of the G substructural units in lignin was also evaluated and again compared to catalyst **7** in both MeOH and DCM (Table 3).

Consistent with our earlier work [30], oxidation of vanillyl alcohol using either symmetric or asymmetric catalysts in MeOH gave quinone yields that were lower than those observed for the corresponding S-model oxidations. Compared to the S-models, vanillyl alcohol has only a single electron-donating -OMe group. Therefore, the phenolic OH bond is stronger, resulting in a lower

Table 2
Arylpiperazine-tethered Co-Schiff base-catalyzed oxidation of syringyl alcohol in DCM.

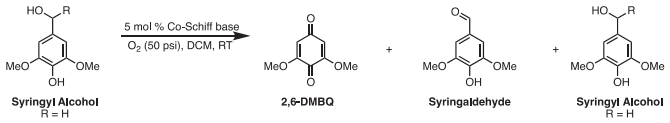

Entry	Catalyst	Substrate	Reaction Time (h)	DMBQ yield (%)[a]	Syringaldehyde yield (%)[a]
1	**7**, asym-NBn	SyOH	18	53	17
2	**10**, asym-Phenethyl	SyOH	18	26	30
3	**13**, sym-Phenethyl	SyOH	18	38	24

Mol % is calculated relative to the substrate.
[a] Yields obtained via ^{1}H NMR integration.

Table 3
Arylpiperazine-tethered Co-Schiff base-catalyzed oxidation of vanillyl alcohol.

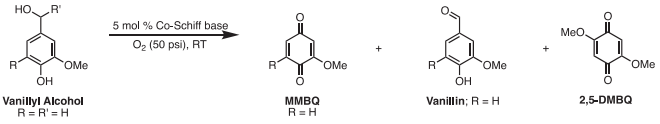

Entry	Catalyst	Solvent	Reaction Time (h)	MMBQ yield (%)[a]	2,5-DMBQ yield (%)[a]	Vanillin yield (%)[b]	Recovered vanillyl alcohol (%)[a]
1	**7**, asym-NBn	DCM	17	59	–	–	2
2	**7**, asym-NBn	MeOH	18	34	5	–	32
3	**9**, asym-diPhMe	DCM	17	48[c]	–	–	10[c]
4	**9**, asym-diPhMe	MeOH	18	32[c]	3[c]	–	22[c]
5	**10**, asym-Phenethyl	DCM	17	42[c]	–	–	33
6	**10**, asym-Phenethyl	MeOH	18	28	5	–	30
7	**13**, sym-Phenethyl	DCM	17	16[b,c]	–	1[c]	38[c]
8	**13**, sym-Phenethyl	MeOH	18	1	–	–	39
9	**11**, sym-NBn	DCM	17	48[c]	–	2[c]	15[c,d]
10	**12**, sym-diPhMe	DCM	17	48[c]	–	–	–
11	**12**, sym-diPhMe	MeOH	18	13[c]	9[c]	–	45[c]

Mol % is calculated relative to the substrate; diPhMe: 1-diphenylmethyl; Phenethyl: 1-phenethyl.
[a] Isolated yield.
[b] Yields obtained via ^{1}H NMR integration.
[c] Denotes the average yields between two different runs.
[d] Combined yield from isolated and ^{1}H NMR integration.

rate of phenoxyl radical formation and thus, a lower yield of MMBQ [62–66]. The baseline oxidation using catalyst **7** provided MMBQ in 59% and 34% yield in DCM and methanol, respectively (Table 3, entries 1 and 2). Asymmetric catalysts **9** and **10** followed the same pattern (Table 3, entries 3–6). Catalyst **13** was the least effective, giving only a 13% yield of MMBQ after 17 h in DCM and negligible amounts in MeOH (Table 3, entries 7 and 8).

In contrast to S models, DCM is a better oxidation solvent than MeOH for oxidation of G models. We speculate that while the MeOH solvent may be sufficiently coordinating to promote oxidation of the more reactive S models, the low reactivity of G models in either solvent allows alternate deactivation reactions to occur, such as the direct reaction of the catalyst with the MeOH solvent to afford non-reactive Co complexes [67]. In DCM, this alternate reaction is eliminated. The reactions still proceed in lower yield than oxidations of S models, but the steric bulk of the complexes also slows catalyst dimerization and deactivation, allowing at least some MMBQ formation to occur.

Although the absolute yields for G model oxidations are lower than the corresponding S model oxidations, there are interesting parallels as a function of substituent size. Catalyst **7** bearing a single N-Bn group gives higher yields with both S (Table 1, entries 1 and 2) and G models (Table 3, entry 1) than the corresponding catalyst **11** bearing two N-benzyl groups (Table 1, entries 9 and 10 and Table 3, entry 9). Both asymmetric and symmetric diPhMe catalysts **9** and **12** show little or no difference in reactivity, and also show reactivity similar to symmetric catalyst **11** (Table 1, entries 9 and 15 and Table 3, entry 9). These results suggest that **9**, **11**, and **12** present a similar steric environment during the oxidation of either S or G substrates. In contrast, the steric environment presented by symmetric catalyst **13** leads to markedly lower yields for oxidation of both S and G models in comparison to all other catalysts.

2.5. Computational studies for the arylpiperazine-tethered Co-Schiff base catalysts

All catalysts and their oxygenated adducts were subjected to computational evaluation. An initial Monte Carlo search was carried out on structures in which the Co-Schiff base, cyclohexyl bridge and *t*-butyl groups were frozen, while allowing the substituents and oxygens (where appropriate) to move. A family of conformers was generated, and the low energy conformation for each was further refined via DFT in Gaussian 16 (see Supplemental Material). These data were then used to examine possible correlations between the structure of low energy conformations and the effectiveness of the catalyst. DFT results may have several local minima, but the Boltzman distribution values for several of the catalyst structures indicate that certain conformations are much more

highly populated than others, suggesting that such geometric orientations may have greater impact on reactivity than others. This assumption is supported by the experimental results from our oxidation, both in this work and earlier work from our group [19,20]. Fig. 4 illustrates the low energy conformations calculated for complexes **7**, **9**, **11** and **12**. The dz^2 orbital energies for these complexes are comparable to other complexes in this series (Fig. 2). For all complexes, we observed little or no change in conformation upon oxygenation, and thus, discussion will focus on the non-oxygenated adducts.

The piperazine adopts a chair conformation in each complex with the substituents on the piperazine nitrogens in the equatorial position. With this orientation, complexes **7**, **9** and **12** display substituents roughly perpendicular to the plane of the Schiff base ligand (e. g., the diPhMe substituent in **9** is positioned at an angle of 112.95° to the Schiff base plane while the two diPhMe substituents in **12** are at angles of 114.65° and 117.12°, respectively). The low energy conformation for **12** also places the substituents on opposite sides of the Schiff base ligand. Complex **11** minimizes in an unusual manner, with one of the N-Bn substituents bending under the plane of the Schiff base ligand.

In this group of catalysts, *asym*-NBn complex **7** catalyzes the oxidation of syringyl alcohol to DMBQ in 71% yield after 18 h in MeOH. Similarly, asymmetric complex **9** affords a 70% yield of DMBQ after 18 h. The effect of adding a second diPhMe-piperazine group appears to have minimal effect on the catalyst effectiveness when compared to the asymmetric catalyst, as **12** converts syringyl alcohol to DMBQ in an almost identical 73% after 18 h. α-Methyl-syringyl alcohol gives DMBQ in 73% yield after 16 h. The reproducibility of yields at both short and long reaction times, however, suggests that any slow quinone consumption path (as suggested for asymmetric catalysts) may be reduced with the simultaneous presence of large substituents on both sides of the catalyst.

Based on these similar yields, we conclude that the NBn and diPhMe groups provide a steric environment similar to the *t*-Bu groups on the periphery of the catalyst. Because the reactions do not require addition of an external axial base, the substituents also provide a steric barrier to catalyst dimerization and subsequent deactivation. Neither the addition of a second phenyl group to the benzylic position of the substituted piperazine (i. e., a diPhMe substituent) nor the presence of a second diPhMe group negatively affects catalyst reactivity when methanol is used as the solvent. Complex **11** exhibits a small, but reproducibly lower yield of DMBQ suggesting that the presence of one N-Bn piperazine in the vicinity of the Co center in the low energy conformer may slightly reduce access to the Co. Further experiments are underway to verify this impact.

Interestingly, asymmetric phenethyl complex **10** minimizes in a unique conformation (Fig. 5). The calculated low energy conformation has the phenethyl group rotated roughly parallel to the face of the catalyst as with complex **11**, but is the result of the piperazine adopting a boat conformation with the nitrogen substituents in an axial orientation.

In contrast to **7** and **9**, which give lower DMBQ yields at longer reaction times, phenethyl complex **10** gives higher yields after 18 h. These observations suggest that the location of the phenethyl under the plane of the ligand provides greater hindrance to non-productive catalyst dimerization or deactivation processes. The source of stabilization for the low energy conformations adopted by both **10** and **11** is not obvious. π-Type interaction between the phenethyl group and the aromatic rings of the Schiff base may be possible, but the calculated distance between the aromatic rings (slightly greater than 4 Å) is on the far edge of typical pi-pi stacking.

Symmetrically substituted phenethyl catalyst **13** gives the lowest oxidation yields for either S or G models in both MeOH and DCM. Computational evaluation of **13** (Fig. 6) reveals significant differences from its asymmetrically substituted counterpart (Fig. 4).

In contrast to the asymmetrically substituted complexes **10** or **11**, neither of the phenethyl groups are rotated toward the plane of the Schiff base ligand. Instead, the calculated low energy conformation orients the substituents away from and to opposite sides of the ligand. Both piperazines retain the chair conformation, with one piperazine placing the nitrogen substituents in the axial position. Surprisingly, however, the other piperazine adopts a conformation placing one nitrogen substituent in the equatorial position and the other in an axial position. The result is that one phenethyl group is approximately parallel to the plane of the Schiff base ligand. We find that this catalyst is markedly less effective in converting syringyl alcohol to DMBQ, affording only 52% yield after 18 h. Similarly, vanillyl alcohol gives only 16% MMBQ upon oxidation in DCM. Based on the computational results, we speculate that the presence of two substituents reduces nonproductive deactivation pathways. Simultaneously, the presence of a piperazine substituent bearing both axial and equatorial groups may allow approach of the large substituent to the Co, further reducing access to the catalytic center and lowering the yield.

3. Conclusions

The steric environment around the Schiff base ligand and the Co have a strong effect on the ability of the catalysts to carry out oxidation of lignin models. The ability of Co-Schiff base catalysts to oxidize lignin models to the corresponding quinones is subject to a balance between catalyst reactivity and catalyst deactivation. With sufficient steric bulk around the periphery of the Schiff base ligand, catalyst deactivation is reduced, allowing oxidations to proceed in

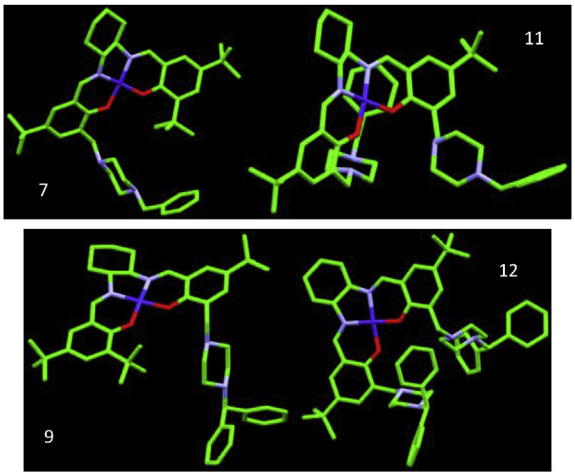

Fig. 4. Low energy conformations of catalysts **7**, **9**, **11** and **12**.

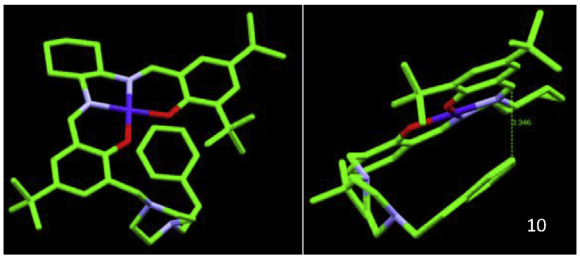

Fig. 5. Low energy conformation of phenethyl complex **10**.

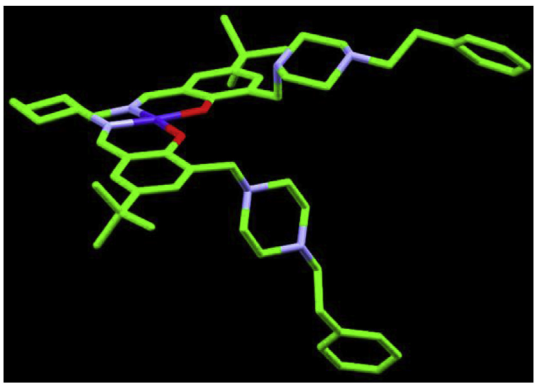

Fig. 6. Low energy conformations of catalyst **13**.

the absence of an added axial ligand, in marked contrast to oxidations using structurally simpler complexes (e. g., **1**).

The reason for this effect is the ability of large substituents to shift the catalyst reactivity/deactivation balance toward the former. At present, the computational results suggest that these effects may be subtle, but important, based on the small energy differences between low energy conformations of the effective catalysts. We find that for S-models, the diPhMe- and NBn-piperazine groups maintain the reactivity of the catalyst system and act similarly to *t*-Bu groups (i. e., Jacobsen-like ligands) on the periphery of the Schiff base ligand. Catalyst **10**, bearing a single phenethyl group, gave excellent yields of quinone from the oxidation of S-models and may have unique qualities as a result of its conformation during reaction. The oxidation of G-models remains more challenging, as these new catalysts gave lower yields of MMBQ than oxidation of the corresponding S-models. Our ongoing work in catalyst design will continue to couple synthetic and computational evaluation to develop systems that will oxidize S and G units with equal facility. Given that lignin composed almost entirely of S units can be obtained from transgenic poplar with increased F5H expression [68], future work will also involve the examination of catalysts **7** and **9**–**12** for the oxidative deconstruction of bioengineered, high-S lignin. The result will be new methodology for the conversion of lignin, which will streamline operation and offer new catalytic routes to biobased chemicals and fuels from renewable carbon.

4. Experimental

4.1. General Information

All reactions were performed under a nitrogen atmosphere unless otherwise stated. Commercially available chemicals (compounds **14**, **15**, **19**, **21,** benzyl bromide, 4-*tert*-butylphenol, dichloromethane, diethyl ether, ethyl acetate, formaldehyde, hexanes, hydrochloric acid, methanol, methylmagnesium bromide, paraformaldehyde, piperazine, potassium iodide, sodium bicarbonate, sodium chloride, syringaldehyde, syringyl alcohol, triethylamine, vanillyl alcohol) were used as received unless otherwise stipulated. Magnesium chloride was dried overnight in a 110 °C oven prior to use. Anhydrous solvents were obtained from either a MBRAUN MB-SPS solvent purification system or used as received from commercial vendors. Symmetric catalyst **11** was synthesized based on our previously reported procedures [19]. Compounds **7**, **26**, **20**, 1-benzylpiperazine, 5-*tert*-butyl-2-hydroxybenzaldehyde, 3-((4-benzylpiperazin-1-yl)methyl)-5-*tert*-butyl-2-hydroxybenzaldehyde, 2-((4-benzylpiperazin-1-yl)methyl)-4-(*tert*-butyl)-6-((*E*)-(((±)-*trans*-2-((*E*)-(3,5-di-*tert*-butyl-2-hydroxybenzylidene)amino)cyclohexyl)imino)methyl)phenol, and 6,6'-((1*E*,1′*E*)-((((±)-*trans*)-cyclohexane-1,2-diyl)bis(azaneylylidene))bis(methaneylylidene))bis(2-((4-benzylpiperazin-1-yl) methyl)-4-(*tert*-butyl)phenol) were synthesized according to published procedures and matched data previously reported [19,30,59,60,69–72]. $Co(OAc)_2 4H_2O$ was dried under vacuum at room temperature for several days prior to use. Molecular sieves (4 Å) were activated in a 110 °C oven prior to use. Analytical thin-layer chromatography (TLC) was performed using glass-backed, pre-coated silica gel 60 F_{254} plates. Flash chromatography was conducted using a Teledyne ISCO CombiFlash® R_f 200 with Teledyne RediSep® R_f or SiliCycle SiliaSep™ (230–400 mesh, 40–63 μm particle size, and 60 Å pore size) silica cartridges. The eluents used are reported in % (v/v). For compounds **22** and **24**, the columns were washed with five column volumes of 1) methanol (to remove water from the column), 2) ethyl acetate, and 3) dichloromethane prior to liquid sample loading.

Melting points were determined using a Fisher-Johns melting point apparatus and are uncorrected. Oxidation procedures were performed in Fisher-Porter tubes under the respective pressure of oxygen denoted in the studies. ^1H and ^{13}C NMR analyses were performed on a either a Varian Unity 400 MHz or a Varian VNMRS 500 MHz instrument; the chemical shifts are given in ppm and are referenced to the appropriate residual nuclei in deuterated solvents. FT-IR spectra were acquired on either a PerkinElmer Spectrum One or PerkinElmer Spectrum Two spectrometer at 4 cm^{-1} resolution and are reported in cm^{-1}. DART-TOF and high-resolution mass spectrometry (HRMS) analyses were obtained on a JEOL AccuTOF-DART™ and an Applied Biosystems QStar Elite HPLC-QTOF mass spectrometer, respectively, at the University of Tennessee Biological and Small Molecule Mass Spectrometry Core. Values are reported as *m*/*z* (relative ratio). Accurate masses were determined for the molecular ion $(M + H)^+$, an acceptable ion, or the neutral species; the results are reported with an error of <3 ppm for DART-TOF and <4 ppm for ESI-MS.

4.2. General procedure for the oxidation of lignin models

CAUTION: The oxidation reactions were performed in thick-walled, glass Fisher-Porter tubes under pressurized oxygen. Though no difficulties were experienced, adequate precautions should be considered when using organic compounds and oxygen above atmospheric pressure. Lignin models were oxidized according to a previously published procedure [19,30]. Briefly, to a Fisher-Porter tube was added 1 equivalent of the lignin model, 0.05 equivalents of Co-Schiff base catalyst, and the appropriate amount of methanol or dichloromethane to make a 0.2 M solution relative to the lignin model substrate. The tube was flushed three times and then pressurized to 50 psi using oxygen. Once pressurized, the reaction was stirred at room temperature for times denoted in Tables 1–3. If significant quantities of yellow solid (quinone) precipitated upon completion of the reaction, the mixture was filtered, and the mother liquor was concentrated under reduced pressure. This residue was analyzed by NMR to determine the amount of any additional quinone. If minimal or no yellow solid was present upon completion of the reaction, the mixture was concentrated under reduced pressure. Purification (silica gel; 0-2-5-10-100% EtOAc:DCM) gave the respective *para*-benzoquinones in yields reported in Tables 1–3

4.3. Computational modeling methodology

All calculations for the study were conducted on the Alabama Supercomputer Network. An initial conformational search was done using a 1000 step Monte Carlo procedure with MMFF

minimization at each step, as implemented in Spartan '16. The Co-salen moiety, cyclohexyl bridge and *t*-butyl groups were frozen, while the substituents and oxygens, where appropriate, were allowed to move. The low energy conformation for each was refined using the M06-L density functional method, the LANL2DZ basis set for the cobalt and the 6-31G(d,p) basis set for carbon, nitrogen, hydrogen and oxygen. The structures were optimized, with frequency calculations for thermal corrections and to insure the identification of a stationary point, and done using the SMD solvation model for ethanol. All DFT calculations were done with Gaussian 16, Revision A.03. These data were then used to examine possible correlations between the structure of low energy conformations and the effectiveness of the catalyst. Final renderings were carried out using Mercury 3.10 (Build 156946).

4.4. Syntheses of catalyst precursors

4.4.1. Synthesis of 3-((4-benzhydrylpiperazin-1-yl)methyl)-5-(tert-butyl)-2-hydroxybenzaldehyde (**17**)

To a round-bottom flask equipped with a stirbar was added potassium iodide (0.1553 g, 0.93 mmol), a solution of compound **16** (1.98 g, 8.73 mmol) in ethyl acetate (22 mL), and a solution of 1-(diphenylmethyl)piperazine (**14**) (3.3410 g, 13.2 mmol) in ethyl acetate (82 mL). The reaction was stirred for 1.6 h at room temperature. Upon completion, the mixture was diluted with dichloromethane, washed with equal volumes of saturated aqueous $NaHCO_3$ (2X), dried over anhydrous Na_2SO_4, and concentrated under reduced pressure. Purification (silica gel; 0-2-5-10-100% EtOAc:DCM) gave **17** as an off-white solid in 43% yield. $R_f = 0.62$ (10% EtOAc:DCM); IR (neat) 2963, 2806, 2762, 1677, 1605, 1479, 1451, 1281, 1236, 1216, 1133, 1004, 971, 896, 850, 758, 744, 708, 693, 605 cm^{-1}; ^1H NMR (400 MHz, $CDCl_3$): δ 10.29 (s, 1H), 7.62 (d, $J = 4$ Hz, 1H), 7.42–7.38 (m, 4H), 7.29–7.24 (m, 5H), 7.20–7.15 (m, 2H), 4.27 (s, 1H), 3.78 (s, 2H), 2.76–2.39 (br, 8H), 1.29 (s, 9H); ^{13}C NMR (100 MHz, $CDCl_3$): δ 192.0, 159.2, 142.3, 141.8, 133.1, 128.5, 127.8, 127.0, 124.9, 122.5, 121.9, 75.9, 59.6, 52.8, 51.4, 34.0, 31.2; DART-TOF Calcd for $C_{29}H_{34}N_2O_2$ $(M + H)^+$: 443.26985, found 443.26883.

4.4.2. Synthesis of 5-(tert-butyl)-2-hydroxy-3-((4-phenethylpiperazin-1-yl)methyl)benzaldehyde (**18**)

To a round-bottom flask equipped with a stirbar was added potassium iodide (0.3712 g, 2.24 mmol), a solution of compound **16** (5.02 g, 22.1 mmol) in ethyl acetate (56 mL), and a solution of 1-phenethylpiperazine (**15**) (6.3 mL, 33.3 mmol) in ethyl acetate (56 mL). The reaction was stirred for 1.5 h at room temperature. Upon completion, the mixture was diluted with an equal volume of dichloromethane, washed with equal volumes of saturated aqueous $NaHCO_3$ (2X), back extracted with an equal volume of dichloromethane (1X), dried over anhydrous Na_2SO_4, and concentrated under reduced pressure. Purification (silica gel; 0-5-20-25-100% EtOAc:DCM) gave **18** as an off-white solid in 30% yield. $R_f = 0.31$, (20% EtOAc:hexanes); IR (neat) 2948, 2847, 2803, 2847, 2762, 1673, 1604, 1474, 1363, 1292, 1220, 1154, 1132, 1114, 1006, 962, 930, 888, 846, 819, 754, 701, 605 cm^{-1}; ^1H NMR (400 MHz, $CDCl_3$): δ 10.34 (s, 1H), 7.64 (d, $J = 2.4$ Hz, 1H), 7.33 (d, $J = 4$ Hz, 1H), 7.31–7.27 (m, 2H), 7.22–7.18 (m, 3H), 3.75 (s, 2H), 2.84–2.77 (m, 4H), 2.68–2.59 (m, 8H), 1.30 (s, 9H); ^{13}C NMR (100 MHz, $CDCl_3$): δ 191.8, 159.2, 141.9, 140.1, 132.9, 128.7, 128.4, 126.1, 124.8, 122.8, 122.1, 60.2, 59.9, 52.9, 52.6, 34.1, 33.6, 31.3; DART-TOF Calcd for $C_{24}H_{32}N_2O_2$ $(M + H)^+$: 381.2542; found 381.25444.

4.5. Synthesis of asymmetric Schiff base ligands

4.5.1. Synthesis of 2-((4-benzhydrylpiperazin-1-yl)methyl)-4-(tert-butyl)-6-((E)-((((±)-trans)-2-(((E)-3,5-di-tert-butyl-2-hydroxybenzylidene)amino)cyclohexyl)imino)methyl)phenol (**22**)

To a round-bottom flask equipped with a stirbar was added (±)-*trans*-1,2-diaminocyclohexane (**19**) (1.2 mL, 9.99 mmol) and anhydrous ethanol (52 mL), and the flask was cooled to 0 °C. Hydrochloric acid (2.0 M in diethyl ether, 5 mL, 10 mmol) was added dropwise, and the solution was stirred for 1 h at room temperature. A solution of 3,5-di-*tert*-butyl-2-hydroxybenzaldehyde (**21**) (2.4079 g, 10.3 mmol) in anhydrous ethanol (52 mL) was added, along with 4 Å MS (3.65 g). After stirring 3.25 h at room temperature, a solution of compound **17** (4.55 g, 10.3 mmol) in anhydrous ethanol (172 mL + heating at 95 °C for complete dissolution) and triethylamine (2.9 mL, 20.8 mmol) was added, and the solution was allowed to stir for 20 h at room temperature. Upon completion, the reaction mixture was concentrated under reduced pressure and purified (silica gel; 2-5-10-15-20-100 EtOAc:DCM; see General Information for column prep instructions). Drying under vacuum at 65 °C for 18 h gave the final product as a yellow solid in 64% yield. mp: 163–166 °C; $R_f = 0.15$ (10% EtOAc:DCM); IR (neat): 2953, 2860, 2806, 2763, 1627, 1451, 1362, 1273, 1174, 1136, 1096, 1031, 1007, 911, 878, 849, 827, 773, 757, 745, 732, 705, 641 cm^{-1}; ^1H NMR (400 MHz, $CDCl_3$): δ 13.68 (s, 1H), 13.42 (br, 1H), 8.29 (s, 1H), 8.26 (s, 1H), 7.40 (d, $J = 8$ Hz, 4H), 7.29 (d, $J = 4$ Hz, 1H), 7.27–7.22 (m, 5H), 7.15 (m, $J = 8$ Hz, 2H), 7.02 (d, $J = 4$ Hz, 1H), 6.97 (d, $J = 4$ Hz, 1H), 4.21 (s, 1H), 3.61 (d, $J = 12$ Hz, 1H), 3.49 (d, $J = 12$ Hz, 1H), 3.36–3.22 (m, 2H), 2.52 (br, 4H), 2.43 (br, 4H), 1.97–1.81 (m, 4H), 1.77–1.64 (m, 2H), 1.50–1.42 (m, 2H), 1.40 (s, 9H), 1.23 (s, 9H), 1.20 (s, 9H); ^{13}C NMR: (100 MHz, $CDCl_3$): δ 165.7, 165.1, 158.0, 157.2, 143.0, 140.4, 139.9, 136.3, 128.4, 128.0, 126.77, 126.7, 126.65, 126.0, 124.4, 76.4, 72.8, 72.2, 56.3, 54.0, 52.0, 34.9, 34.0, 33.8, 33.4, 33.1, 31.43, 31.35, 29.4, 24.3; DART-TOF Calcd for $C_{50}H_{66}N_4O_2$ $(M + H)^+$: 755.5264; found 755.52542.

4.5.2. Synthesis of 2,4-di-tert-butyl-6-((E)-((((±)-trans)-2-(((E)-5-(tert-butyl)-2-hydroxy-3-((4-phenethylpiperazin-1-yl)methyl)benzylidene)amino)cyclohexyl)imino)methyl)phenol (**23**)

To a round-bottom flask equipped with a stirbar was added compound **19** (0.35 mL, 2.91 mmol) and anhydrous ethanol (15 mL), and the flask was cooled to 0 °C. Hydrochloric acid (2.0 M in diethyl ether, 1.5 mL, 3.0 mmol) was added dropwise, and the solution was stirred for 1 h at room temperature. A solution of compound **21** (0.6758 g, 2.88 mmol) in anhydrous ethanol (15 mL) was added. After stirring 2.5 h at room temperature, a solution of compound **18** (1.1035 g, 2.90 mmol) in anhydrous ethanol (98 mL and then heated at 80 °C to fully dissolve the salicylaldehyde) and triethylamine (0.82 mL, 5.88 mmol) was added, and the solution was stirred for 21 h at room temperature. Upon completion, the reaction mixture was concentrated under reduced pressure and purified (silica gel; 5-10-20-40-50-100% EtOAc:hexanes). Drying under vacuum at 65 °C for 5 h gave the final product as a solid in 60% yield. mp: 102–104 °C; $R_f = 0.18$ (40% EtOAc:hexanes); IR (neat): 2950, 2862, 2808, 1627, 1456, 1362, 1272, 1173, 1133, 1095, 1034, 1012, 908, 878, 818, 772, 731, 699, 644 cm^{-1}; ^1H NMR (400 MHz, $CDCl_3$): δ 13.70 (br, 1H), 13.44 (br, 1H), 8.31 (s, 1H), 8.27 (s, 1H), 7.33 (d, $J = 4$ Hz, 1H), 7.31 (d, $J = 4$ Hz, 1H), 7.30–7.25 (m, 2H), 7.21–7.16 (m, 3H), 7.05 (d, $J = 4$ Hz, 1H), 6.99 (d, $J = 4$ Hz, 1H), 3.64 (d, $J = 16$ Hz, 1H), 3.54 (d, $J = 16$ Hz, 1H), 3.39–3.23 (m, 2H), 2.83–2.76 (m, 2H), 2.62–2.54 (m, 10H), 1.98–1.82 (m, 4H), 1.79–1.64 (m, 2H), 1.51–1.42 (m, 2H), 1.41 (s, 9H), 1.24 (s, 9H), 1.23 (s, 9H); ^{13}C NMR (100 MHz, $CDCl_3$): δ 165.7, 165.1, 158.0, 157.3, 140.5, 140.4, 140.0, 136.4, 130.7, 128.7, 128.3, 126.7, 126.0, 125.97, 117.84, 117.80, 72.8, 72.3, 60.6, 56.3, 53.2, 53.1, 35.0, 34.1, 33.8, 33.7, 33.4, 33.1, 31.44, 31.37, 29.4, 24.33, 24.27;

DART-TOF: Calcd for $C_{45}H_{64}N_4O_2$ $(M + H)^+$: 693.51075; found 693.51178.

4.6. Synthesis of sym-Schiff base ligands

4.6.1. General

Arylpiperazine salicylaldehyde (2 equivalents) was dissolved in anhydrous ethanol (with gentle heating for complete dissolution). Compound **19** (1 equivalent) was added, and the reaction was stirred for 24 h at room temperature. Upon completion, the reaction mixture was concentrated under reduced pressure, taken up in dichloromethane, dried over anhydrous Na_2SO_4, and concentrated under reduced pressure again.

4.6.2. 6,6'-((1E,1'E)-((((±)-trans)-cyclohexane-1,2-diyl) bis(azaneylylidene))bis(methaneylylidene))bis(2-((4-benzhydrylpiperazin-1-yl)methyl)-4-(tert-butyl)phenol) (**24**)

Purification (silica gel; 12-50-100% EtOAc:DCM; see General Information for column prep instructions), followed by drying under vacuum at 70 °C for 5 h, gave the final product as a yellow solid in 48% yield. mp: 135–138 °C; $R_f = 0.12$ (50% EtOAc:DCM); IR (neat): 2955, 2933, 2900, 2862, 2807, 2762, 1627, 1450, 1272, 1221, 1136, 1076, 1006, 850, 825, 745, 704, 639 cm^{-1}; ^1H NMR (400 MHz, $CDCl_3$): δ 13.38 (br, 2H), 8.26 (s, 2H), 7.43–7.39 (m, 8H), 7.31 (d, $J = 4$ Hz, 2H), 7.28–7.22 (m, 8H), 7.18–7.13 (m, 4H), 7.03 (d, $J = 4$ Hz, 2H), 4.22 (s, 2H), 3.63 (d, $J = 16$ Hz, 2H), 3.49 (d, $J = 16$ Hz, 2H), 3.31–3.26 (m, 2H), 2.53 (br, 8H), 2.44 (br, 8H), 1.93–1.82 (m, 4H), 1.74–1.63 (m, 2H), 1.49–1.40 (m, 2H), 1.21 (s, 18H). ^{13}C NMR: (100 MHz, $CDCl_3$): δ 165.0, 157.2, 143.0, 140.4, 130.7, 128.4, 127.9, 126.8, 124.5, 117.1, 76.3, 72.7, 56.3, 53.5, 52.0, 33.8, 33.3, 31.4, 24.2; DART-TOF: Calcd for $C_{64}H_{78}N_6O_2$ $(M + H)^+$: 963.62395; found 963.62520.

4.6.3. 6,6'-((1E,1'E)-((((±)-trans)-cyclohexane-1,2-diyl) bis(azaneylylidene))bis(methaneylylidene))bis(4-(tert-butyl)-2-((4-phenethylpiperazin-1-yl)methyl)phenol) (**25**)

Purification (silica gel; 50–100% EtOAc:hexanes), followed by drying under vacuum at 60 °C for 20 h gave the final product as a yellow solid in 93% yield. mp: 141–144 °C; $R_f = 0.12$ (100% EtOAc); IR (neat): 2935, 2808, 1628, 1459, 1362, 1262, 1133, 1093, 1012, 818, 801, 730, 698 cm^{-1}; ^1H NMR (400 MHz, $CDCl_3$): δ 13.42 (br, 2H), 8.29 (s, 2H), 7.35 (d, $J = 4$ Hz, 2H), 7.30–7.25 (m, 4H), 7.20–7.16 (m, 6H), 7.07 (d, $J = 4$ Hz, 2H), 3.66 (d, $J = 16$ Hz, 2H), 3.54 (d, $J = 12$ Hz, 2H), 3.33–3.28 (m, 2H), 2.83–2.77 (m, 4H), 2.63–2.54 (m, 20H), 1.94–1.83 (m, 4H), 1.74–1.65 (m, 2H), 1.50–1.40 (m, 2H), 1.25 (m, 18H); ^{13}C NMR (100 MHz, $CDCl_3$): δ 164.9, 157.2, 140.5, 140.4, 130.7, 128.7, 128.3, 126.7, 126.0, 124.3, 117.8, 72.7, 60.6, 56.2, 53.2, 53.1, 33.9, 33.7, 33.3, 31.4, 24.2; DART-TOF: Calcd for $C_{54}H_{74}N_6O_2$ $(M + H)^+$: 839.59515; found 839.59710.

4.7. Synthesis of asymmetric Co-Schiff base complexes

4.7.1. General

In a pressure tube equipped with a stirbar, asymmetric arylpiperazine-tethered Schiff base ligand (1 equivalent) was dissolved in anhydrous methanol. Then, $Co(OAc)_2 4H_2O$ (1 equivalent) was dissolved in anhydrous methanol and added to the tube. The cap was affixed, and the reaction was heated at reflux for 4 h. Following reflux, the precipitate was collected via filtration and washed using cold methanol.

4.7.2. Co-Schiff base complex **9**

Drying under vacuum at 80 °C for 4 h provided catalyst **9** as an orange solid in 21% yield. IR (neat): 2951, 2904, 2867, 2809, 1594, 1528, 1429, 1315, 1255, 1135, 1004, 837, 748, 705, 557 cm^{-1}; DART-TOF: Calcd for $C_{50}H_{64}CoN_4O_2$ $(M + H)^+$: 812.44395; found 812.44539.

4.7.3. Co-Schiff base complex **10**

Drying under vacuum at 75 °C for 4 h provided catalyst **10** as a brick red solid in 45% yield. IR (neat): 2945, 2902, 2866, 2800, 1592, 1525, 1426, 1321, 1253, 1155, 1132, 1043, 926, 873, 837, 787, 740, 695, 640 cm^{-1}; DART-TOF Calcd for $C_{45}H_{62}CoN_4O_2$ $(M + H)^+$: 750.42578; found 750.42704.

4.8. Synthesis of symmetric Co-Schiff base complexes

4.8.1. General

In a pressure tube, equipped with a stirbar, symmetric arylpiperazine-tethered Schiff base ligand (1 equivalent) was dissolved in anhydrous methanol. Then, $Co(OAc)_2 4H_2O$ (1 equivalent) was dissolved in anhydrous methanol and added to the tube, the cap was affixed, and the reaction was allowed to reflux for 4 h.

4.8.2. Synthesis of Co-Schiff base complex **12**

Following reflux, the orange precipitate was collected via filtration and washed with cold methanol. Drying under vacuum at 65 °C for 5 h provided catalyst **12** as an orange solid in 59% yield. IR (neat): 2959, 2810, 1614, 1594, 1537, 1451, 1326, 1265, 1222, 1150, 1132, 1078, 1046, 1007, 937, 847, 749, 697, 641, 609 cm^{-1}; HRMS (ESI-MS): Calcd for $C_{64}H_{76}CoN_6O_2$ $(M)^{+\cdot}$: 1019.5361; found 1019.5392.

4.8.3. Synthesis of Co-Schiff base catalyst 13

Following reflux and cooling to room temperature, the brick red solution was concentrated under reduced pressure to obtain a brown viscous liquid, which was taken up in Et_2O and concentrated under reduced pressure once again. The brown solid was isolated via filtration and washed with hexanes. Drying under vacuum at 65 °C for 4 h provided catalyst **13** as a dark brown solid in 96% yield. IR (neat): 2953, 2871, 1570, 1395, 1319, 1044, 699 cm-1; HRMS (ESI-MS): Calcd for C54H72CoN6O2 (M + H)+: 896.51024; found 896.5110.

Acknowledgements

We would like to thank the Center for Direct Catalytic Conversion of Biomass to Biofuels (C3Bio), an Energy Frontier Research Center (EFRC) that is funded by the United States Department of Energy, Office of Science, Basic Energy Sciences, award DE-SC0000997. We would also like to thank Mr. Ernesto C. Zuleta for thoughtful discussion regarding the mechanistic pathways for the phenolic oxidation and the UT Biological and Small Molecule Mass Spectrometry Core for DART-TOF and HRMS measurements.

Appendix A. Supplementary data

Supplementary data to this article can be found online at https://doi.org/10.1016/j.tet.2019.04.059.

References

[1] R. Rinaldi, R. Jastrzebski, M.T. Clough, J. Ralph, M. Kennema, P.C.A. Bruijnincx, B.M. Weckhuysen, Angew. Chem. Int. Ed. 55 (2016) 8164–8215.
[2] O. Gordobil, R. Moriana, L.M. Zhang, J. Labidi, O. Sevastyanova, Ind. Crops Prod. 83 (2016) 155–165.
[3] J.J. Bozell, J.E. Holladay, D. Johnson, J.F. White, Pacific Northwest, National Laboratory, Richland, WA, 2007.
[4] R.E. Key, J.J. Bozell, ACS Sustain. Chem. Eng. 4 (2016) 5123–5135.
[5] J. Zakzeski, P.C.A. Bruijnincx, A.L. Jongerius, B.M. Weckhuysen, Chem. Rev. 110 (2010) 3552–3599.
[6] R. Vanholme, B. Demedts, K. Morreel, J. Ralph, W. Boerjan, Plant Physiol. 153

(2010) 895–905.
[7] J.J. Bozell, C.J. O'Lenick, S. Warwick, J. Agric. Food Chem. 59 (2011) 9232–9242.
[8] G. Vazquez, G. Antorrena, J. Gonzalez, S. Freire, J. Wood Chem. Technol. 17 (1997) 147–162.
[9] P. Prinsen, J. Rencoret, A. Gutierrez, T. Liitia, T. Tamminen, J.L. Colodette, M.A. Berbis, J. Jimenez-Barbero, A.T. Martinez, J.C. del Rio, Ind. Eng. Chem. Res. 52 (2013) 15702–15712.
[10] J.B. Li, G. Gellerstedt, K. Toven, Bioresour. Technol. 100 (2009) 2556–2561.
[11] J. Tao, O. Hosseinaei, L. Delbeck, P. Kim, D.P. Harper, J.J. Bozell, T.G. Rials, N. Labbé, RSC Adv. 6 (2016) 79228–79235.
[12] A. Wu, B.O. Patrick, E. Chung, B.R. James, Dalton Trans. 41 (2012) 11093–11106.
[13] J.M. Nichols, L.M. Bishop, R.G. Bergman, J.A. Ellman, J. Am. Chem. Soc. 132 (2010) 12554–12555.
[14] A.G. Sergeev, J.F. Hartwig, Science 332 (2011) 439–443.
[15] J.Y. He, C. Zhao, J.A. Lercher, J. Am. Chem. Soc. 134 (2012) 20768–20775.
[16] J. Zakzeski, P.C.A. Bruijnincx, B.M. Weckhuysen, Green Chem. 13 (2011) 671–680.
[17] S.K. Hanson, R.T. Baker, Acc. Chem. Res. 48 (2015) 2037–2048.
[18] A. Rahimi, A. Azarpira, H. Kim, J. Ralph, S.S. Stahl, J. Am. Chem. Soc. 135 (2013) 6415–6418.
[19] B. Biannic, J. Bozell, J. Org. Lett. 15 (2013) 2730–2733.
[20] B. Biannic, J.J. Bozell, T. Elder, Green Chem. 16 (2014) 3635–3642.
[21] J.J. Bozell, Top. Curr. Chem. 353 (2014) 229–256.
[22] M. Wang, L.H. Li, J.M. Lu, H.J. Li, X.C. Zhang, H.F. Liu, N.C. Luo, F. Wang, Green Chem. 19 (2017) 702–706.
[23] J.M. Pepper, H. Hibbert, J. Am. Chem. Soc. 70 (1948) 67–71.
[24] S. Van den Bosch, T. Renders, S. Kennis, S.F. Koelewijn, G. Van den Bossche, T. Vangeel, A. Deneyer, D. Depuydt, C.M. Courtin, J.M. Thevelein, W. Schutyser, B.F. Sels, Green Chem. 19 (2017) 3313–3326.
[25] T.H. Parsell, B.C. Owen, I. Klein, T.M. Jarrell, C.L. Marcum, L.J. Haupert, L.M. Amundson, H.I. Kenttamaa, F. Ribeiro, J.T. Miller, M.M. Abu-Omar, Chem. Sci. 4 (2013) 806–813.
[26] H. Luo, I.M. Klein, Y. Jiang, H.Y. Zhu, B.Y. Liu, H.I. Kenttamaa, M.M. Abu-Omar, ACS Sustain. Chem. Eng. 4 (2016) 2316–2322.
[27] Q. Song, F. Wang, J.Y. Cai, Y.H. Wang, J.J. Zhang, W.Q. Yu, J. Xu, Energy Environ. Sci. 6 (2013) 994–1007.
[28] A.J. Ragauskas, G.T. Beckham, M.J. Biddy, R. Chandra, F. Chen, M.F. Davis, B.H. Davison, R.A. Dixon, P. Gilna, M. Keller, P. Langan, A.K. Naskar, J.N. Saddler, T.J. Tschaplinski, G.A. Tuskan, C.E. Wyman, Science 344 (2014) 709–719.
[29] D.R. Robert, M. Bardet, G. Gellerstedt, E.L. Lindfors, J. Wood Chem. Technol. 4 (1984) 239–263.
[30] J.J. Bozell, B.R. Hames, D.R. Dimmel, J. Org. Chem. 60 (1995) 2398–2404.
[31] D. Cedeno, J.J. Bozell, Tetrahedron Lett. 53 (2012) 2380–2383.
[32] I. Sasaki, D. Pujol, A. Gaudemer, Inorg. Chim. Acta 134 (1987) 53–57.
[33] A. Pui, C. Dobrota, J.-P. Mahy, J. Coord. Chem. 60 (2007) 581–595.
[34] A. Pui, I. Berdan, A. Cascaval, Rev. Roum. Chem. 45 (2000) 331–335.
[35] A. Zombeck, R.S. Drago, B.B. Corden, J.H. Gaul, J. Am. Chem. Soc. 103 (1981) 7580–7585.
[36] B.B. Corden, R.S. Drago, R.P. Perito, J. Am. Chem. Soc. 107 (1985) 2903–2907.
[37] G.T. Musie, M. Wei, B. Subramaniam, D.H. Busch, Inorg. Chem. 40 (2001) 3336–3341.
[38] E.E. Podlesny, P.J. Carroll, M.C. Kozlowski, Org. Lett. 14 (2012) 4862–4865.
[39] A. Nishinaga, H. Tomita, J. Mol. Catal. 7 (1980) 179–199.
[40] P.G. Cozzi, Chem. Soc. Rev. 33 (2004) 410–421.
[41] D. Chen, A.E. Martell, Y.Z. Sun, Inorg. Chem. 28 (1989) 2647–2652.
[42] H.M. van Dort, H.J. Geursen, Recl. Trav. Chim. Pays-Bas 86 (1967) 520–526.
[43] L.H. Vogt, J.G. Wirth, H.L. Finkbeiner, J. Org. Chem. 34 (1969) 273–277.
[44] D.L. Tomaja, L.H. Vogt, J.G. Wirth, J. Org. Chem. 35 (1970) 2029 (&).
[45] R.A. Sheldon, J.K. Kochi, Metal Catalyzed Oxidations of Organic Compounds, Academic Press, New York, 1981.
[46] C. Floriani, F. Calderazzo, J. Chem. Soc. A (1969) 946–953.
[47] D. Chen, A.E. Martell, Inorg. Chem. 26 (1987) 1026–1030.
[48] A. Pui, J.P. Mahy, Polyhedron 26 (2007) 3143–3152.
[49] A. Pui, C. Policar, J.P. Mahy, Inorg. Chim. Acta 360 (2007) 2139–2144.
[50] P. Zanello, R. Cini, A. Cinquantini, P.L. Orioli, J. Chem. Soc. Dalton (1983) 2159–2166.
[51] C. Daul, J. Weber, Helv. Chim. Acta 65 (1982) 2486–2497.
[52] E.G. Samsel, J.K. Kochi, Inorg. Chem. 25 (1986) 2450–2457.
[53] F. Basolo, B.M. Hoffman, J.A. Ibers, Acc. Chem. Res. 8 (1975) 384–392.
[54] T. Elder, J.J. Bozell, D. Cedeno, Phys. Chem. Chem. Phys. 15 (2013) 7328–7337.
[55] P.J. Pospisil, D.H. Carsten, E.N. Jacobsen, Chem. Eur. J. 2 (1996) 974–980.
[56] W. Zhang, J.L. Loebach, S.R. Wilson, E.N. Jacobsen, J. Am. Chem. Soc. 112 (1990) 2801–2803.
[57] B. Gao, X. Li, R.L. Duan, Q. Duan, Y.H. Li, X. Pang, H.J. Zhuang, X.S. Chen, RSC Adv. 5 (2015) 29412–29419.
[58] W. Chaładaj, P. Kwiatkowski, J. Jurczak, Tetrahedron Lett. 49 (2008) 6810–6811.
[59] M. Holbach, X.L. Zheng, C. Burd, C.W. Jones, M. Weck, J. Org. Chem. 71 (2006) 2903–2906.
[60] E.J. Campbell, S.T. Nguyen, Tetrahedron Lett. 42 (2001) 1221–1225.
[61] Zuleta, E.; Bozell, J.; Elder, T., *manuscript in preparation*.
[62] J.A. Howard, K.U. Ingold, Can. J. Chem. 41 (1963) 1744–1751.
[63] A. Borghese, R. Merényi, J. Penelle, P. Pigeolet, H.G. Viehe, J. Prakt. Chem. 334 (1992) 563–569.
[64] E.F. Caldin, S.P. Dagnall, M.K.S. Mak, D.N. Brooke, Faraday Discuss. Chem. Soc. 74 (1982) 215–228.
[65] F.G. Bordwell, J. Cheng, J. Am. Chem. Soc. 113 (1991) 1736–1743.
[66] M.M. Suryan, S.A. Kafafi, S.E. Stein, J. Am. Chem. Soc. 111 (1989) 4594–4600.
[67] A. Nishinaga, T. Kondo, T. Matsuura, Chem. Lett. 14 (1985) 905–908.
[68] S.K. Huntley, D. Ellis, M. Gilbert, C. Chapple, S.D. Mansfield, J. Agric. Food. Chem. 51 (2003) 6178–6183.
[69] D.E. Bergbreiter, P.L. Osburn, C.M. Li, Org. Lett. 4 (2002) 737–740.
[70] P. Meier, F. Broghammer, K. Latendorf, G. Rauhut, R. Peters, Molecules 17 (2012) 7121–7150.
[71] Q. Wang, C. Wilson, A.J. Blake, S.R. Collinson, P.A. Tasker, M. Schroder, Tetrahedron Lett. 47 (2006) 8983–8987.
[72] M.W. Fennie, E.F. DiMauro, E.M. O'Brien, V. Annamalai, M.C. Kozlowski, Tetrahedron 61 (2005) 6249–6265.